



This article appeared in a journal published by Elsevier. The attached copy is furnished to the author for internal non-commercial research and education use, including for instruction at the authors institution and sharing with colleagues.

Other uses, including reproduction and distribution, or selling or licensing copies, or posting to personal, institutional or third party websites are prohibited.

In most cases authors are permitted to post their version of the article (e.g. in Word or Tex form) to their personal website or institutional repository. Authors requiring further information regarding Elsevier's archiving and manuscript policies are encouraged to visit:

<http://www.elsevier.com/copyright>



Contents lists available at ScienceDirect

Surface Science

journal homepage: www.elsevier.com/locate/susc

Enhanced photodesorption by vibrational pre-excitation: Quantum model simulations for Cs/Cu(1 1 1)

Dominik Kröner*, Stefan Klinkusch, Tillmann Klamroth

Institut für Chemie, Theoretische Chemie, Universität Potsdam, Karl-Liebknecht-Strasse 24-25, D-14167 Potsdam, Germany

ARTICLE INFO

Available online 9 July 2008

Keywords:

Empirical models and model calculations
Desorption induced by electronic transition (DIET)

Desorption induced by photon stimulation

ABSTRACT

We present quantum model simulations for the laser-induced desorption of Cs from Cu(1 1 1) induced by a charge transfer from the Cu surface state to an unoccupied resonance state of the Cs-adsorbate. Based on empirical two-state model potentials along the Cs–Cu distance quantum nuclear dynamics were performed including electronic relaxation to account for the ultrashort lifetime of the resonance state. In order to increase the negligible desorption yield obtained from direct UV excitation the system was vibrationally pre-excited by a THz-laser pulse. Using an “jumping” wavepacket incoherent averaging scheme we calculated the desorption probability with respect to the time evolution of a vibrational wavepacket on the electronic ground state. The desorption probability is significantly increased for short Cs–Cu distances, but it is almost negligible for the stretched Cs–Cu bond. Vibrational pre-excitation enhances the photodesorption of Cs from Cu(1 1 1), but only if the timing of the laser-induced charge transfer is chosen correctly.

© 2008 Elsevier B.V. All rights reserved.

1. Introduction

Photodesorption of adspecies from solid surfaces is a key element in photo-catalysis, electrophotochemistry and surface nanochemistry. One of the best studied photo-reactions is the so-called desorption induced by electronic transition (DIET) [1]. The desorption from metal surfaces induced by ultrashort UV/vis laser pulses is typically substrate-mediated, i.e. in the DIET-limit a single electron within the metal substrate is transferred to a short-lived excited state, a so-called resonance. Exemplary, this occurs either by *direct* excitation of the electron to an unoccupied adsorbate state or *indirectly* by excitation of the electron inside the metal, creating a “hot” electron, and subsequent tunneling of the electron to the adsorbate. In either case the resonance decays rapidly while the electron returns to the metal surface. In addition, the adsorbate feels forces in the electronic excited state that are absent in the ground state. If the resonance lifetime is sufficiently long for the adsorbate to accumulate enough energy in the excited state it will desorb on the ground state potential.

In the case of indirect excitation via “hot” metal electrons a simultaneous theoretical treatment of electron and nuclear motion is required: for NO/Pt(1 1 1) we performed coupled electron–nuclear quantum dynamics based on a two-dimensional model potential by Harris et al. [2] applying a highly efficient numerical scheme to propagate the wavepacket in a problem-adapted diabatic basis [3].

While for NO/Pt(1 1 1) the direct excitation of the resonance state is rather inefficient with respect to the desorption yield [3], systems with weak coupling between resonance state and bulk electronic states (i.e. with resonance lifetimes longer than a few fs) should allow for more efficient control of the desorption probability by direct laser excitation.

In exceptional cases the direct electronic excitation using UV/vis lasers is possible even for metals, as e.g. in Cs/Cu(1 1 1) where a direct transition from an occupied surface state (SS) of the Cu substrate to an anti-bonding state (A) of the Cs-adsorbate succeeds with photons of approximately 3 eV [4], see Fig. 1a (arrow 1). This corresponds to an electron transfer from the metal to the adsorbate, i.e. a neutralization of the charge since the adsorbate exists as Cs⁺-ion in the ground state, see Fig. 1b (arrow 1). The neutral excited potential energy curve is repulsive and has a comparatively long lifetime, in the order of tens of femtoseconds [4–6], cf. Fig. 1a and b (arrow 2). Thus, according to a Menzel–Gomer–Redhead scenario [7] desorption or at least vibrational excitation of the adsorbate is expected.

Cs/Cu(1 1 1) is especially attractive for both theoreticians [8–12] and experimentalists [4–6,13–15] since the unexpected long lifetime of low-lying excited adsorbate states allows to experimentally monitor the subsequent nuclear motion of the adatom away from the surface in real time by time-resolved two-photon photo-emission (TR-2PPE) [4,14]. Gauyacq et al. explained the long lifetime in comparison to other adsorbate/metal systems by the specific electronic structure of Cu(1 1 1): Both the SS and A states are located within a large projected band gap. As a consequence

* Corresponding author.

E-mail address: kroener@uni-potsdam.de (D. Kröner).

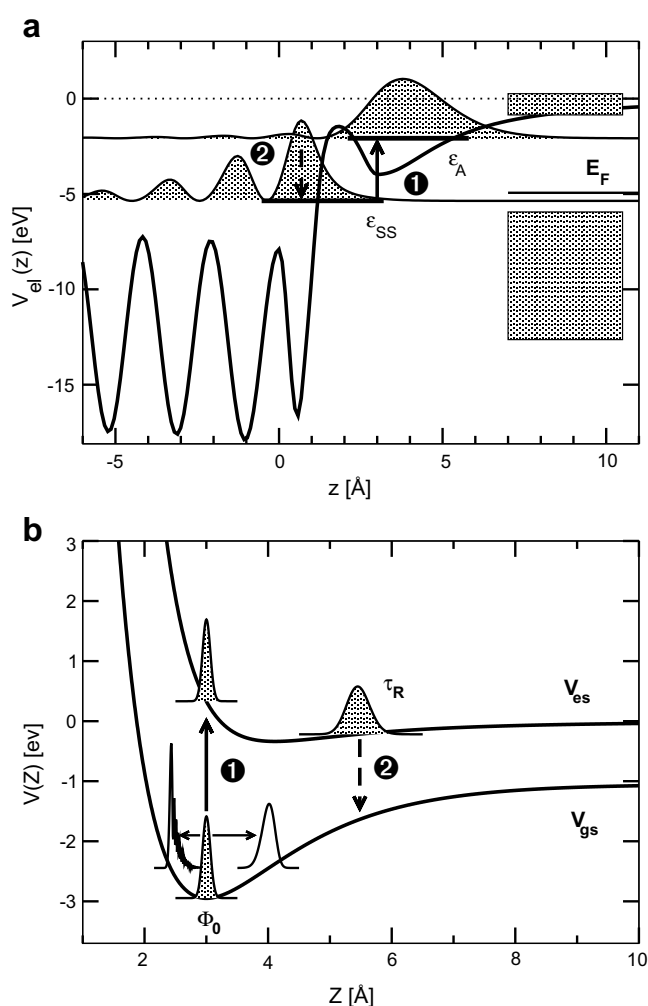


Fig. 1. Laser-induced charge transfer **1** and subsequent relaxation **2** for Cs/Cu(111): (a) Section of the one-electron model potential along the surface normal z of the Cu slab [16]. SS and A-state are indicated by horizontal lines for their energies $\epsilon_{SS/A}$ and by their respective eigenfunctions $|\varphi_{SS/A}|^2$. The blocks indicate the band of bulk states and of the “Rydberg series”, respectively. (b) Nuclear potential energy curves for the electronic ground V_{gs} and the excited state V_{es} along the Cs–Cu distance Z . Φ_0 (patterned) is the vibrational ground state wave function. For the incoherent averaging Φ_0 is vertically transferred up to V_{es} (solid arrow) and propagated for each residence time τ_R before it is placed back onto V_{gs} due to energy relaxation (dashed arrow). The horizontal arrows indicate the vibrational motion of the ground state wavepacket (blank) after THz laser pulse excitation.

the A state couples only weakly to the bulk electronic states, thus reducing the amount of inelastic electron–electron scattering, and resonant charge transfer [9,10]. The observed lifetime of the anti-bonding resonance state for Cs/Cu(111) is about $\tau_{res} \approx 15 \pm 6$ fs according to Ref. [5] (at $T = 300$ K) or $\tau_{res} \approx 50$ fs according to Ref. [6] (at $T = 50$ K). Borisov et al. used an one-electron wavepacket propagation in combination with stationary many particle theory to calculate the lifetime of Cs on Cu(111) [9,10], resulting in $\tau_{res} = 28$ fs.

Recently, we theoretically investigated the charge transfer process in Cs/Cu(111) using model potentials [16]. In passing we note that the calculation of reliable ground and electronic excited state potential energy surfaces for adsorbates on solid surfaces from first principles is a challenging task [17,18]. In particular for electronic excited states of metals on metals surfaces the determination of the continuum of metal excitations is due to its high computational effort not feasible. Then again, model

potentials fitted to experimental observables are very useful to simulate photodesorption on metal [3] and metal oxide surfaces [19,20].

Due to the weak electronic coupling in Cs/Cu(111) we treated electronic and nuclear motion separately in our model simulations [16]: The electronic problem, i.e. the laser-induced charge transfer as well as the subsequent relaxation, was modeled using a modified effective one-electron potential $V_{el}(z)$ after Chulkov et al. [8] where z describes the motion of the single active electron parallel to the surface normal, see Fig. 1a. For low Cs-coverage the electron model potential reproduces experimentally obtained energies of the surface state (SS) and of the adsorbate state (A) quite well. Further, the lifetime of the resonance state was determined to be 32 fs, using an eigenfunction overlap criterion [21]. In addition, transition dipole moments $\langle \varphi_n | -ez | \varphi_m \rangle$ were calculated with $|\varphi_m\rangle$ being the electronic eigenfunctions of the potential $V_{el}(z)$ obtained from the one-electron model. Afterwards the electron dynamics were simulated. Electric fields in accordance with experimentally applied ones [4] lead to very small excitation rates. Still, laser pulses retrieved from optimal control theory (OCT) [22,23] gave rise to a population of more than 90% in the target state even if energy dissipation was included.

These optimized laser pulses were still effective if nuclear motion was considered within a two-state model of nuclear model potentials $V_{gs}(Z)$ and $V_{es}(Z)$, with Z being the Cs–Cu distance, see Fig. 1b. However, the desorption yield obtained from an incoherent averaging scheme starting from the vibrational ground state is vanishingly low. If the calculation starts, however, from a shifted vibrational ground state wave function, i.e. Φ_0^{ss} is placed to the classical turning points of the potential at higher energy, to simulate vibrational pre-excitation, the desorption probability is noticeable increased depending on the mean position of the shifted wave function [16].

The concept of enhancing desorption by an IR + UV/vis strategy, i.e. first vibrationally excite the adsorbate, and then desorb it by electronic excitation, has been investigated theoretically [24–28] and experimentally [29–31]. In most studies the vibrational preparation was accomplished by surface heating [29–31] or modeled by choosing a particular eigenstate of the adsorption mode as an initial state [24–27]. Thiel et al., for instance, showed in quantum model simulations and experiments that an increase of the surface temperature leads to an increase of the non-thermal desorption of NO from $\text{Cr}_2\text{O}_3(0001)$ [31]. While in the theoretical simulations of Ref. [31] the vibrational pre-excitation was modeled as an incoherent, thermal mixture of the vibrational eigenstates Nakagami et al. employed a coherent excitation of the NO-surface vibration in NO/Pt(111) using an IR pulse obtained from optimal control theory [28]. The optimal IR pulse prepares the NO molecule such that it moves towards the Pt(111) surface at the moment of the electronic excitation and, thereby, increases the desorption probability according to an Antoniewicz scenario [32].

In this paper, we present nuclear dynamics propagations within our nuclear potentials model [16] for analytical THz laser pulses of different mean intensities which produce a vibrationally excited coherent wavepacket in the electronic ground state. Further, the desorption probability due to an subsequent vertical electronic excitation is calculated as a function of the time when this excitation takes place, i.e. depending on the time evolution of the vibrational wavepacket in the electronic ground state. In this way we are able to gain a detailed insight of the effect of vibrational pre-excitation on the enhancement of the desorption yield.

The paper is structured as follows: Section 2 covers the nuclear model potentials as well as the theoretical techniques applied in this work. In Section 3 we discuss the results obtained from quantum nuclear dynamical simulations. The paper concludes with Section 4.

2. Theory

The nuclear model potentials are adopted from Ref. [16]. They were constructed in accordance with the results obtained from our one-electron model potential [16] and reproduce experimental findings. The ionic electronic ground state (Cs^+/Cu^-) is given by a Morse potential converging asymptotically to the difference between the Cs ionization energy IE_{Cs} and the Cu work function Φ_{Cu} [33]:

$$V_{\text{gs}}(Z) = -D_e + D_e[1 - e^{-a(Z-Z_0)}]^2 + (IE_{\text{Cs}} - \Phi_{\text{Cu}}). \quad (1)$$

D_e is the ground state desorption energy of 1.9 eV [15], Z_0 the Cs–Cu equilibrium distance (3 Å [34]) and a determines the Cs–Cu vibrational frequency (see below). Although the potential (1) does not properly account for the long-range Coulomb forces, it is appropriate for the questions addressed here.

The neutral electronic excited state (Cs^0/Cu^0) is modeled by an exponentially decaying function for the short-range repulsive and a van der Waals term for the long-range attractive forces [33]:

$$V_{\text{es}}(Z) = V_0 \cdot e^{-b(Z-Z_0)} - \frac{C_3}{Z^3} \quad \text{for } Z \geq 2.0a_0, \quad (2)$$

with $b = 1.0071a_0^{-1}$. The vertical excitation energy is taken from the electronic model $\Delta E(Z_0) = \varepsilon_A(Z_0) - \varepsilon_{\text{SS}}(Z_0) = 3.28$ eV (with z_0 being the Cs^+ core – image plane distance) [16] which is within the correct range of experimental values for the case of low Cs coverage [5,35]. The slope of the excited state potential at the Frank–Condon point Z_0 was predicted by Petek and coworkers to be -1.9 eV/Å [15]. With the vertical excitation energy $\Delta E(Z_0)$ and the predicted slope at Z_0 , the parameters V_0 and C_3 can be calculated by solving $V_{\text{es}}(Z_0) = V_{\text{gs}}(Z_0) + \Delta E(Z_0)$ and $\frac{d}{dZ}V_{\text{es}}(Z_0) = -1.9$ eV/Å. All parameters of the nuclear potentials are listed in Table 1. The nuclear potential energy curves are depicted in Fig. 1b.

The vibrational eigenfunctions Φ_i^σ of the system are obtained by solving the time-independent Schrödinger equation:

$$\hat{H}_0^\sigma \Phi_i^\sigma(Z) = E_i^\sigma \Phi_i^\sigma(Z) \quad \text{with} \quad \hat{H}_0^\sigma(Z) = -\frac{\hbar^2}{2M} \frac{d^2}{dZ^2} + V_\sigma(Z), \quad (3)$$

for the ground ($\sigma = \text{gs}$) and electronic excited state ($\sigma = \text{es}$), using the Fourier Grid Hamiltonian method [36] with 4096 grid points for $2.0a_0 \leq Z \leq 42a_0$. The following limiting case is considered: The Cu surface is rigid and the Cs-atom scatters elastically on the surface, i.e. $M = m_{\text{Cs}} = 242271.78 m_e$. Simulations of the excited state nuclear dynamics [16] suggest that this assumption is reasonable for the slope of the excited state potential at the Franck–Condon point used here. If the recoil of the surface atoms was considered a smaller mass M would be required which on his part leads to a time-dependent displacement after electronic excitation being far too fast compared to the experimental value given in Ref. [15]. For a detailed discussion the reader is referred to Ref. [16].

The initial state of the quantum dynamical simulations is the lowest vibrational eigenfunction Φ_0^{gs} of V_{gs} , see Fig. 1b. The dynamics are described by the time-dependent Schrödinger equation:

$$i\hbar \frac{\partial}{\partial t} \begin{pmatrix} \Psi_{\text{es}}(t) \\ \Psi_{\text{gs}}(t) \end{pmatrix} = \begin{pmatrix} \hat{H}_0^{\text{es}} & 0 \\ 0 & \hat{H}_0^{\text{gs}} - \mu_{\text{gs}}(Z)E(t) \end{pmatrix} \begin{pmatrix} \Psi_{\text{es}}(t) \\ \Psi_{\text{gs}}(t) \end{pmatrix}. \quad (4)$$

Table 1

Parameters of the ground V_{gs} and the electronic excited state V_{es} potential energy curves, see Eqs. (1) and (2)

D_e [eV]	IE_{Cs} [eV]	Φ_{Cu} [eV]	$a[a_0^{-1}]$	$Z_0 [a_0]$
1.9	3.89	4.94	0.38	5.67
V_0 [eV]	$b[a_0^{-1}]$	C_3 [eVÅ ³]	$\Delta E(Z_0)$ [eV]	$\frac{d}{dZ}V_{\text{es}}(Z_0)$ [eV/Å]
1.73813	1.0071	256.68	3.28	-1.9

The off-diagonal elements of the Hamiltonian in Eq. (4) are zero, because electronic transitions are treated as instantaneous excitations/de-excitations (see below). As a consequence wavepackets on ground $\Psi_{\text{gs}}(t)$ and excited $\Psi_{\text{es}}(t)$ state were propagated independently.

For the vibrational pre-excitation of the system in the ground state laser fields of the following analytical form were applied for $|t - t_d| \leq \text{fwhm}$:

$$E(t) = E^0 \cdot \cos(\omega(t - t_d)) \cdot \sin^2\left(\frac{\pi(t - t_d)}{2\text{fwhm}} + \frac{\pi}{2}\right), \quad (5)$$

with amplitude E^0 , frequency ω and full width at half maximum fwhm. The \sin^2 -envelope function reaches its maximum at t_d . The dipole moment as a function of the Cs–Cu distance Z is obtained according to the one-electron model: $\mu_{\text{gs}}(Z) = 2(Z - \Delta)e$, where Δ is the distance between the Cu surface and the image plane [16].

In order to investigate the effect of a laser-induced vibrational pre-excitation on the desorption probability the following approach was employed: (i) A THz laser pulse was generated to effectively excite vibrational motion in the electronic ground state. (ii) A “jumping” wavepacket approach is applied to simulate the electronic excitation and subsequent relaxation in order to calculate the desorption probability in the ground state at the end of the process. Step (ii) is performed during the time evolution of the vibrationally excited ground state wavepacket for each time t_i on a equidistant time grid. As a result we obtain a time-resolved desorption probability curve with respect to the time delay between IR and UV excitation, which allows to investigate the efficiency of vibrational pre-excitation.

For step (i) the time-dependent Schrödinger equation for the electronic ground state, cf. Eq. (4), is solved by the split operator method [37] in grid representation (see above) using a time step of 0.1 fs.

For step (ii) the incoherent averaging scheme for N quantum trajectories with excited state residence times τ_{R_n} ($n = 1, \dots, N$) proposed by Gadzuk [38] was applied. In this method, the expectation values of a desired observable, here the desorption probability P_{des} , are weighted by an exponential factor and averaged over all N trajectories:

$$\bar{P}_{\text{des}}(t) = \frac{\sum_{n=1}^N P_{\text{des}}(t; \tau_{R_n}) \cdot e^{-\tau_{R_n}/\tau_{\text{res}}}}{\sum_{n=1}^N e^{-\tau_{R_n}/\tau_{\text{res}}}}, \quad (6)$$

where τ_{res} (32 ps) is the lifetime of the anti-bonding resonance obtained from the electron model [16]. To retrieve $P_{\text{des}}(t; \tau_{R_n})$, initially, the ground state wavepacket $\Psi_{\text{gs}}(t)$ at time t is vertically transferred to the excited state potential V_{es} by transforming the wavefunction in position space into the eigenstate basis $\{\Phi_i^{\text{es}}\}$ of the excited state Hamiltonian \hat{H}_0^{es} . On V_{es} the wavepacket is, then, quasi-analytically propagated to the corresponding residence time τ_{R_n} , see Fig. 1b, i.e. the wavefunction at τ_{R_n} is directly computed from the initial coefficients in the eigenstate representation of \hat{H}_0^{es} . Finally, the wavepacket is vertically transferred back onto the ground state potential V_{gs} by projecting it on the eigenstate basis $\{\Phi_i^{\text{gs}}\}$ of the ground state Hamiltonian \hat{H}_0^{gs} . In this eigenstate basis the desorption probability $P_{\text{des}}(t; \tau_{R_n})$ is calculated as the sum of populations in all states with a total energy of more than -1.05 eV ($IE_{\text{Cs}} - \Phi_{\text{Cu}}$), i.e. the part of the wavepacket that populates states above the ground state desorption energy, see Eq. (1). Finally, the desorption probabilities of the individual quantum trajectories $P_{\text{des}}(t; \tau_{R_n})$ are averaged according to the Gadzuk-scheme (6). $N = 150$ quantum trajectories for residence times of $\tau_{R_n} = n \cdot \Delta\tau_R$ were calculated with $n = 1, 2, \dots, 150$ and $\Delta\tau_R = 5$ fs; convergence was checked with respect to N and τ_{R_N} .

3. Results

First, a few-cycle THz laser pulse was generated to vibrationally excite the Cs–Cu bond starting from the ground state wave function Φ_0^{gs} . The laser frequency was tuned to the transition energy between the ground and first excited vibrational eigenstate $\hbar\omega = E_1^{\text{gs}} - E_0^{\text{gs}} = 7.8$ meV (1.89 THz). Vibrations in the THz regime are in fact characteristic for Cs adsorbed on transition metals: Petek et al. suggest 8 meV, or 1.93 THz ($T = 300$ K) to 6.5 meV, or 1.57 THz ($T = 0$ K) for Cs/Cu(111) [15], and Watanabe et al. stated 9.5 meV, or 2.3 THz for Cs/Pt(111) [39].

The laser pulse induces a ladder climbing, i.e. a vibrational wavepacket is created, see Fig. 1b. This is due to the relative small decrease of energy level spacing with increasing potential energy (anharmonicity parameter $\chi_e = \hbar\sqrt{2D_e a^2/M}/4D_e \approx 0.001$) compared to the broad frequency width of the fs-laser pulse. Laser amplitude E^0 (2 GV/m) and pulse duration (fwhm = $t_d = 625$ fs) were chosen such that an increase of the vibrational energy by 0.5 eV is achieved. This corresponds to the same amount of vibrational excess energy as considered in Ref. [16] using a displaced vibrational ground state wave function. Also the maximal (4.00 Å) and minimal (2.44 Å) position expectation values within the first 5 ps of the propagation are in close agreement with the assumptions in Ref. [16]. The time evolution of the electric field $E(t)$ and the position expectation value $\langle Z \rangle_{\text{gs}}(t)$ of the ground state wavepacket $\Psi_{\text{gs}}(t)$ are shown in Fig. 2.

Second, during the time evolution of the vibrational ground state wavepacket $\Psi_{\text{gs}}(t)$ the system is probed at time t_i by an instantaneous UV laser pulse that induces the electronic excitation. While the excited state decays the wavepacket returns to the ground state. If it has accumulated enough kinetic energy on the excited state potential, it can desorb on the ground state potential.

The Gadzuk-averaged desorption probability \bar{P}_{des} is calculated as a function of the time t_i , when the instantaneous electronic excitation is triggered, with $t_i = i \cdot \Delta t$ for $i = 0, 1, \dots, 1000$ and $\Delta t = 5$ fs. The resulting time-resolved desorption spectrum $\bar{P}_{\text{des}}(t_i)$ is depicted in Fig. 3a. The spectrum shows peaks approximately every 620 fs corresponding to the vibration frequency of the ground state wavepacket of ~ 1.6 THz which is lower than the transition frequency of 1.89 THz due to the anharmonicity of the potential for high energies. Three main observations are made:

(a) The desorption probability \bar{P}_{des} reaches its maxima shortly after the position expectation value of the ground state wave function $\langle Z \rangle_{\text{gs}}(t)$ has reached its minima corresponding to the inner turning point of the wavepacket (≈ 2.4 Å), i.e. the shortest

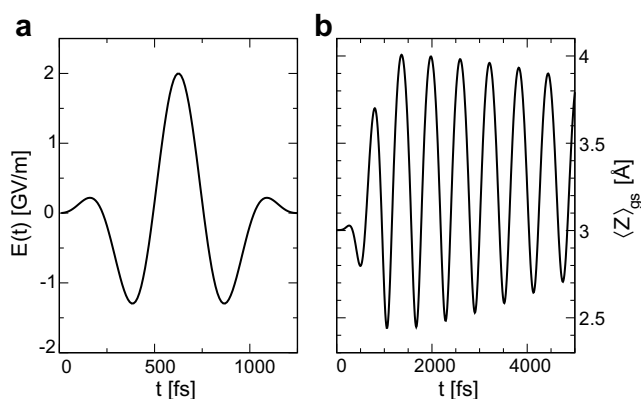


Fig. 2. Laser-induced vibrational pre-excitation for Cs/Cu(111): Time evolution of: (a) the electric field $E(t)$ of the THz laser pulse, and (b) the position expectation value of the ground state wavepacket $\langle Z \rangle_{\text{gs}}(t)$.

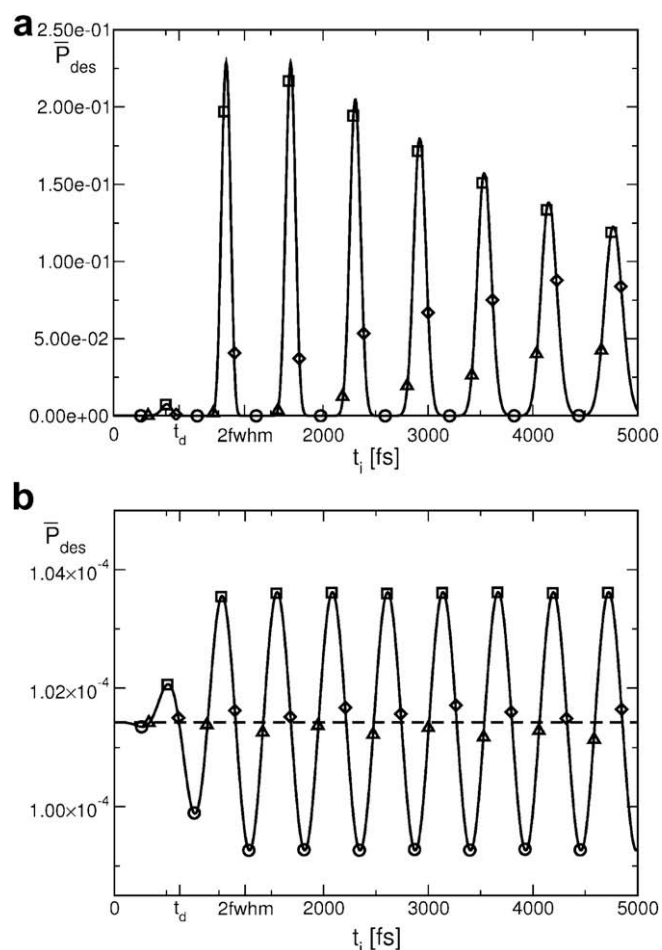


Fig. 3. Averaged desorption probability \bar{P}_{des} as a function of the instantaneous UV excitation time t_i . The system is vibrationally pre-excited by a THz laser pulse of 2 fwhm pulse duration with a mean peak intensity of: (a) 0.5 TW/cm² or (b) 0.5 MW/cm². The circles indicate times, where the time-dependent position expectation value $\langle Z \rangle_{\text{gs}}(t)$ has a maximum, the squares indicate times at which $\langle Z \rangle_{\text{gs}}(t)$ has a minimum. The corresponding times for the time-dependent momentum expectation value $\langle p \rangle_{\text{gs}}(t)$ are indicated by diamonds (maxima) and triangles (minima).

Cs–Cu distance. At first glance this seems surprising, because the ground state momentum expectation value $\langle p \rangle_{\text{gs}}(t)$ is zero at the turning points, and the distance the Cs-atom has to overcome in order to desorb is much larger as if the system was excited at its outer turning point (≈ 4.0 Å). Yet, the slope of the excited state potential V_{es} is much steeper at $Z = 2.4$ Å than at Z_0 or even at $Z = 4.0$ Å. Therefore, after electronic excitation of $\Psi_{\text{gs}}(t)$ at its inner turning point the system accumulates much more kinetic energy on the excited state potential than it does in the case of an excitation of the vibrational ground state function Φ_0^{gs} , see Ref. [16]. For long Cs–Cu distances, see Fig. 3a, \bar{P}_{des} becomes minimal because of the minimum of V_{es} around $Z \approx 4.0$ Å, preventing the wavepacket to gain sufficient kinetic energy.

(b) The maximal desorption probability decreases with time t_i while the peaks broaden. This reflects the broadening of the vibrational ground state wavepacket with time.

(c) The maxima of the peaks of \bar{P}_{des} appear slightly later than the minima of $\langle Z \rangle_{\text{gs}}(t)$, indicated by squares in Fig. 3a. Here, the direction in which the wavepacket is moving in the ground state is decisive. Right after the wavepacket has reached its inner turning point its momentum points toward longer Cs–Cu distances. During the following instantaneous electronic

excitation the momentum of the wavepacket is conserved and enhances the acceleration of wavepacket on V_{es} towards increasing Z . This positive momentum transfer can be better observed at the peak shoulders. The diamonds in Fig. 3a, indicating the maxima of $\langle p \rangle_{\text{gs}}(t)$, are located at higher \bar{P}_{des} than the triangles, indicating the minima of $\langle p \rangle_{\text{gs}}(t)$, with respect to the peak center: Momenta pointing away from the surface result in higher desorption probability than momenta pointing in the opposite direction.

Note that, the maximal desorption probability of about 0.23 is slightly lower than the value calculated in Ref. [16]. This is due to the fact that in Ref. [16] the desorption probability was obtained from the vibrational ground state wave function ϕ_0^{gs} shifted to $Z = 2.425 \text{ \AA}$ which is more compact (than a wavepacket with the same potential energy), i.e. it behaves more like a classical particle. The investigated vibrationally excited wavepacket $\Psi_{\text{gs}}(t)$, in contrast, is broader in Z with a higher probability $|\Psi_{\text{gs}}(Z)|^2$ for larger Z -values which in turn “feel” weaker forces on V_{es} .

The mean peak intensity ($\bar{I} = \frac{1}{2} \epsilon_0 c |E^0|^2$) of the applied laser pulse is with about 0.5 TW/cm^2 far too high for experimental realization. Therefore, a second laser pulse was generated (not shown) by decreasing the amplitude of the original pulse by a factor 1000 to $E^0 = 0.002 \text{ GV/m}$ which corresponds to an experimental more feasible mean peak intensity of about 0.5 MW/cm^2 . The resulting time-resolved desorption spectrum is shown in Fig. 3b. The overall desorption probability is much smaller than in the previous case because the amplitude of the Cs–Cu oscillation is very small ($\approx Z_0 \pm 0.8 \text{ m\AA}$). In contrast to the high intensity pulse \bar{P}_{des} is now oscillating around an average value of about 1.014×10^{-4} with the transition frequency of 1.89 THz due to the quasi-harmonicity of the vibration close to the minimum of the ground state potential. Here, the slope of the excited state potential at the Franck–Condon region has only a small, yet noticeable, effect on the desorption probability: while effect (a) can still be observed, effect (b) disappeared in the observed time domain, because the oscillation frequency is near-harmonic. Also effect (c) is much weaker because the difference between minimal and maximal momentum is much smaller than in the case of the high intense laser pulse. Still, a small momentum transfer is also observed for the low intensity pulse, see Fig. 3b.

4. Conclusions

Based on our empirical nuclear model potentials [16] we calculated the desorption probability for Cs from Cu(111) as a function of the time evolution of the vibrationally pre-excited Cs–Cu bond, in order to predict when the UV excitation is most efficient. For a high desorption yield the electronic excitation must be triggered when the vibrating Cs–Cu bond is shortest because of the steep slope of the excited state potential at small Cs–Cu distances.

The vibrational pre-excitation was achieved by few-cycle THz laser pulses adjusted to the properties of the system. In the case of a very intense laser field, resulting in a highly vibrationally excited Cs–Cu bond, the desorption probability depends not only on the position expectation value of the wavepacket in the ground state, but also on its momentum expectation value. This momentum conservation was also found in the case of vibrational pre-excitation using a pulse of experimentally available field intensity, yet to a much smaller extent. However, in the here applied model the electronic transitions are treated as instantaneous processes, perfectly preserving position and momentum of the initial wave function. Then again, the electronic excitation is typically very short compared to the vibrational motion in the ground state. Furthermore, laser control strategies utilizing momentum transfer in

an electronic transition have proven to be successful for selective bond breaking [40]. Therefore, an efficient momentum transfer from ground to electronic excited state induced by a selective ultrashort UV laser pulses should enhance the desorption yield.

The generation of vibrationally excited wavepackets in the ground state is possible not only using THz laser fields but can also be accomplished by a UV/vis pump–dump mechanism via an electronic excited state. However, to generate a noticeable vibrational excitation in the ground state the lifetime of the electronic excited state must be sufficiently long for the adsorbate to accumulate enough kinetic energy before relaxation. But the longer the wavepacket evolves in the electronic excited state the more it will dephase during its relaxation to the ground state which eventually decreases the chances for an efficient second UV excitation. Since for Cs/Cu(111) the pulse duration of the UV laser inducing the electronic excitation is of about the order of the lifetime of the resonance state this strategy is a challenging task.

Acknowledgements

We wish to thank Professor P. Saalfrank for fruitful discussions. Financial support by the Deutsche Forschungsgemeinschaft (Schwerpunktprogramm 1093, Sonderforschungsbereich 450, and Project No. KR 2942/1) is gratefully acknowledged.

References

- [1] F.M. Zimmermann, W. Ho, Surf. Sci. Rep. 22 (1995) 127.
- [2] S. Harris, S. Holloway, G.R. Darling, J. Chem. Phys. 102 (1995) 8235.
- [3] T. Klamroth, D. Kröner, P. Saalfrank, Phys. Rev. B 72 (2005) 205407.
- [4] H. Petek, M.J. Weida, H. Nagano, S. Ogawa, Science 288 (2000) 1402.
- [5] M. Bauer, S. Pawlik, M. Aeschlimann, Phys. Rev. B 60 (1999) 5016.
- [6] S. Ogawa, H. Nagano, H. Petek, Phys. Rev. Lett. 82 (1999) 1931.
- [7] D. Menzel, R. Gomer, J. Chem. Phys. 41 (1964) 3311; P.A. Redhead, Can. J. Phys. 42 (1964) 886.
- [8] E.V. Chulkov, V.M. Silkin, P.M. Echenique, Surf. Sci. 437 (1999) 330.
- [9] A.G. Borisov, J.P. Gauyacq, A.K. Kazansky, E.V. Chulkov, V.M. Silkin, P.M. Echenique, Phys. Rev. Lett. 86 (2001) 488.
- [10] A.G. Borisov, J.P. Gauyacq, E.V. Chulkov, V.M. Silkin, P.M. Echenique, Phys. Rev. B 65 (2002) 235434.
- [11] A.G. Borisov, A.K. Kazansky, J.P. Gauyacq, Phys. Rev. B 64 (2001) 201105.
- [12] J.P. Gauyacq, A.K. Kazansky, Phys. Rev. B 72 (2005) 045418.
- [13] H. Petek, H. Nagano, M.J. Weida, S. Ogawa, J. Phys. Chem. A 104 (2000) 10234.
- [14] H. Petek, H. Nagano, M.J. Weida, S. Ogawa, J. Phys. Chem. A 105 (2001) 6767.
- [15] H. Petek, S. Ogawa, Annu. Rev. Phys. Chem. 53 (2002) 507.
- [16] D. Kröner, T. Klamroth, M. Nest, P. Saalfrank, Appl. Phys. A 88 (2007) 535.
- [17] D. Kröner, I. Mehdaoui, H.-J. Freund, T. Klüner, Chem. Phys. Lett. 415 (2005) 150.
- [18] I. Mehdaoui, D. Kröner, M. Pykavy, H.-J. Freund, T. Klüner, Phys. Chem. Chem. Phys. 8 (2006) 1584.
- [19] C. Bach, T. Klüner, A. Gross, Appl. Phys. A 78 (2004) 231.
- [20] C. Bach, C. Carogno, A. Gross, Israel J. Chem. 45 (2005) 46.
- [21] T. Fauster, W. Steinmann, in: P. Halevi (Ed.), Photonic Probes of Surfaces, vol. 347, Elsevier, Amsterdam, 1995. (Chapter 8).
- [22] S. Shi, H. Rabitz, J. Chem. Phys. 92 (1990) 364.
- [23] W. Zhu, J. Botina, H. Rabitz, J. Chem. Phys. 108 (1998) 1953.
- [24] P. Saalfrank, R. Baer, R. Kosloff, Chem. Phys. Lett. 230 (1994) 463.
- [25] P. Saalfrank, R. Kosloff, J. Chem. Phys. 105 (1996) 2441.
- [26] P. Saalfrank, T. Klamroth, Ber. Bunsenges. Phys. Chem. 99 (1995) 1347.
- [27] P. Saalfrank, G.K. Paramonov, J. Chem. Phys. 107 (1997) 10723.
- [28] K. Nakagami, Y. Ohtsuki, Y. Fujimura, Chem. Phys. Lett. 360 (2002) 91.
- [29] D. Menzel, Surf. Sci. 14 (1969) 340.
- [30] Q.-S. Xin, X.-Y. Zhu, Chem. Phys. Lett. 265 (1997) 259.
- [31] S. Thiel, T. Klüner, M. Wilde, K. Al-Shamery, H.-J. Freund, Chem. Phys. 228 (1998) 185.
- [32] P.R. Antoniewicz, Phys. Rev. B 21 (1980) 3811.
- [33] B. Hellsing, D.V. Chakarov, L. Österlund, V.P. Zhdanov, B. Kasemo, J. Chem. Phys. 106 (1997) 982.
- [34] S.Å. Lindgren, L. Walldén, R. Rundgren, P. Westrin, J. Neve, Phys. Rev. B 28 (1983) 6707.
- [35] S.Å. Lindgren, L. Walldén, Phys. Rev. B 45 (1992) 6345.
- [36] C.C. Marston, G.G. Balint-Kurti, J. Chem. Phys. 91 (1989) 3571.
- [37] M.D. Feit, J.A. Fleck Jr., J. Chem. Phys. 78 (1983) 301.
- [38] J.W. Gadzuk, Surf. Sci. 342 (1995) 345.
- [39] K. Watanabe, N. Takagi, Y. Matsumoto, Chem. Phys. Lett. 366 (2002) 606.
- [40] N. Elghobashi, P. Krause, J. Manz, M. Oettel, Phys. Chem. Chem. Phys. 5 (2003) 4806.